JMEPEG (2011) 20:219–222
DOI: 10.1007/s11665-010-9674-5

1059-9495/$19.00

Characterization of High-Frequency Induction Brazed Magnesium Alloy Joint with an Al-Mg-Zn Filler Metal

Li Ma, Dingyong He, Xiaoyan Li, and Jianmin Jiang

(Submitted December 30, 2009; in revised form March 11, 2010)

In this paper, a novel Al-Mg-Zn filler metal was designed to join magnesium alloy AZ31B plates by means of high-frequency induction brazing in argon gas shield condition. The microstructure and the mechanical properties of the brazed joint were investigated. The experimental results showed that the brazed joint contained large amount of α-Mg and β-$Mg_{17}(Al, Zn)_{12}$ phases. The homogeneous $Mg_{32}(Al, Zn)_{49}$ phase in the original filler metal was consumed due to the intensive alloying during the brazing process. The results indicate that the shear strength of the brazed joint is 35 MPa. The fracture morphology of the brazed joint exhibits intergranular fracture mode, and the fracture originates from the hard β-$Mg_{17}(Al, Zn)_{12}$ phase.

Keywords brazing, filler metal, fracture, magnesium alloy, mechanical properties

1. Introduction

Magnesium alloys have been widely used in various fields such as aerospace and transportation vehicles due to their high-specific strength, low density, good damping capacity, easy-casting forming, and recycling (Ref 1, 2). In order to further expand the application of magnesium alloys, joining processes such as friction stir welding (Ref 3-5), tungsten inert gas welding (Ref 6-11), vacuum diffusion welding (Ref 12), reactive brazing (Ref 13), laser beam welding (Ref 14-17), and electron beam welding (Ref 18, 19) have been applied to the magnesium alloys. Among them, brazing is advantageous in the manufacturing component with complex shapes, such as heat exchangers, condensers, and sealed containers. Some investigations on the brazing of Mg/Al dissimilar materials and similar magnesium alloys have been done (Ref 13, 20-23). It was addressed that to develop a filler metal with lower melting point for magnesium alloy joining is crucial and study on the microstructure and mechanical property of the brazed joint is also important. In this paper, the brazing of magnesium alloy AZ31B plates was investigated with a novel Al-Mg-Zn filler metal. The microstructure, microhardness, and shear strength of the brazed joint were examined, and the fracture morphology was also observed. It is expected that the results provide a valuable basis for further development on the of magnesium alloy brazing technology.

Li Ma, Dingyong He, Xiaoyan Li, and **Jianmin Jiang**, College of Materials Science and Engineering, Beijing University of Technology, Beijing 100124, P.R. China. Contact e-mail: mali2050@emails.bjut.edu.cn.

2. Experimental Procedure

The base metal is a wrought magnesium alloy AZ31B plate with dimension of 80 mm × 24 mm × 3.3 mm. Its chemical composition is as follows: Al 3.0 wt.%, Zn 1.0 wt.%, Mn 0.3 wt.%, Si 0.1 wt.%, and Mg as the balance. The phase constitution determined by x-ray diffraction (XRD) is a homogeneous α-Mg solid-solution containing Al and Zn elements. The solidus and liquidus temperatures of the alloy are 566 and 627 °C, respectively.

The preparation of the Al-Mg-Zn filler metal is conducted in a crucible electrical resistance furnace at 700 °C under the protection of argon gas. The melting filler metal is performed in a steel mold. The chemical composition determined by x-ray fluorescence (XRF) is as follows: Al 58.2 wt.%, Mg 26.7 wt.%, and Zn 15.1 wt.%.

Prior to brazing, the specimens were degreased in acetone, and the oxide films on the surfaces of both the magnesium alloy AZ31B and the Al-Mg-Zn filler metal were removed by manual grinding with SiC paper up to 600 grit. In order to further remove oxide film and prevent the cleaned joint from oxidation in the brazing, flux QJ201 in form of powder is selected in the experiment, which has a constituent is as follows: KCl 50 wt.%, LiCl 32 wt.%, NaF 10 wt.%, and $ZnCl_2$ 8 wt.%. The melting temperature range of the flux is 460-620 °C. High-frequency induction heating device was used in the experiment. The heating power and working frequency were 25 and 50 kHz, respectively. During the brazing, the flux were spread on the surface of filler metal with a dimension of 24 mm × 3 mm × 3 mm, which was set on the edge of overlapping position of bottom specimens. The overlapping length and clearance of the brazed joint are 6 and 0.4 mm, respectively, in the experiment. Schematic drawing of the brazed specimens are presented in Fig. 1. The specimens were heat treated at 520-550 °C for 120 s. During the brazing process, argon gas was maintained to protect the samples from oxidation throughout the experiment. When the temperature of brazing chamber was cooled to room temperature, the brazed specimens were taken out, and the residual flux on was removed with a brush in

clean water. The brazed specimens were then cross-sectioned by a cutting machine. To observe the microstructure of the brazed joint, 4 vol.% nitric acid alcoholic solution was applied to etch the samples surface. The microstructure, fracture morphology, and phase constitution in the brazing region were investigated by a scanning electron microscope (SEM) with energy dispersive spectrometer (EDS) and an x-ray diffractometer. The microhardness of the formation phases in the brazing region was measured by means of a Vickers hardness tester with a load of 0.5 N for 15 s indenting time. The chemical composition of the brazing region was analyzed by an XRF spectrum analytical apparatus. The mechanical properties of the overlapped joint were tested by a MTS 810 materials test system.

3. Results and Discussion

3.1 Microstructure of the Filler Metal

The phase constitution of the Al-Mg-Zn filler metal determined by XRD is a homogeneous $Mg_{32}(Al, Zn)_{49}$ phase, as shown in Fig. 2. These phases are shown in Fig. 3, presenting the coarse $Mg_{32}(Al, Zn)_{49}$ crystal grains display on the black matrix with same phase composition. The solidus and liquidus temperatures of the filler metal determined by differential thermal analysis (DTA) are 447 and 462 °C, respectively, as shown in Fig. 4. The DTA curve of the filler metal also indicated that the filler metal has a narrow melting zone, which is beneficial for the magnesium alloy brazing.

3.2 Microstructure of the Brazed Joint

The secondary electron image of the brazed joint is presented in Fig. 5(a). The coarse phase is distributed at boundaries of the grains in the brazing region, and no porosity or tiny crack can be seen in the brazed joint. An apparent boundary between the diffusion zone and the base metal AZ31B was formed, which has a diffusion zone with width of 6-7 μm. The EDS analysis indicates that the matrix of the diffusion zone is α-Mg with a small amount of Zn and Al solid solution. This is favorable since the solid solution strengthens the brazed joint. The EDS line scan analysis (Fig. 5b) shows that the relative content of Mg element in the diffusion zone decreases gradually from the base metal to the brazing metal. It is due to diffusion of Zn and Al elements in the Al-Mg-Zn filler metal. The farther distance is, the less capability of diffusion is.

3.3 Phase Constitution of the Brazing Metal

The results of XRF indicate that the chemical composition of the brazing metal consists of Mg 80.1 wt.%, Al 16.4 wt.%, and Zn 3.5 wt.%. Compared with the original chemical composition of the Al-Mg-Zn filler metal, a complex exchange between the molten filler metal and the base metal happened in the process of the brazing. As a result, the content of Mg element greatly increases, and the relative content of Al and Zn elements decreases in the brazing region. The interaction between the molten filler metal and the base metal leads the Al-based fill metal to be transformed into Mg-based brazing metal. XRD pattern of the brazing metal is presented in Fig. 6,

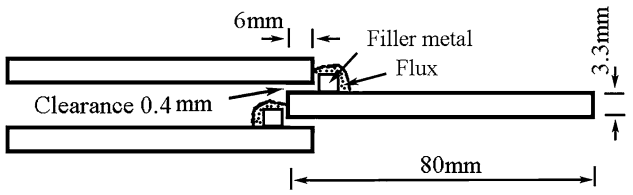

Fig. 1 Schematic drawing of the brazed specimens

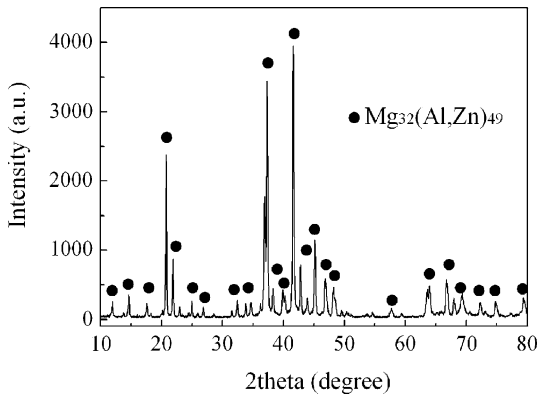

Fig. 2 XRD pattern of the filler metal

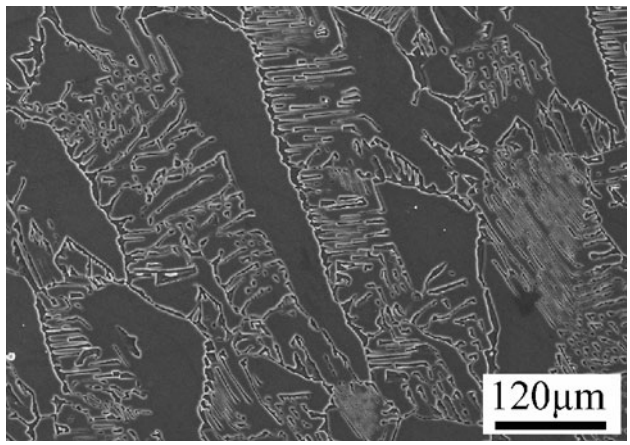

Fig. 3 SEM secondary electron image of the filler metal

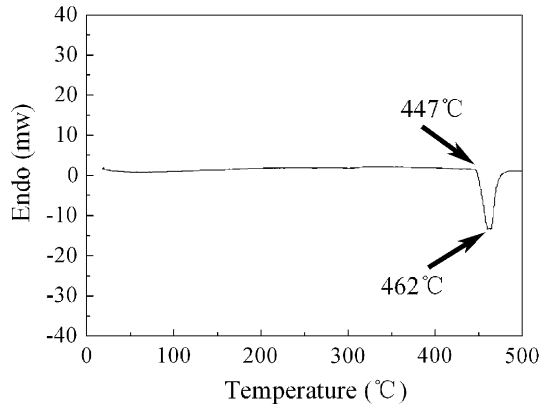

Fig. 4 DTA curve of the filler metal

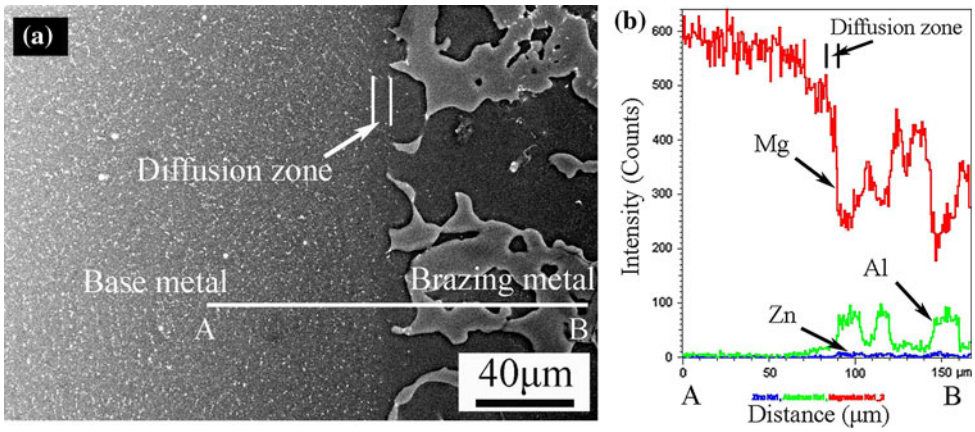

Fig. 5 (a) SEM secondary electron image of the brazed joint and (b) the EDS line scan showing the magnesium, aluminum, and zinc distribution along AB in (a)

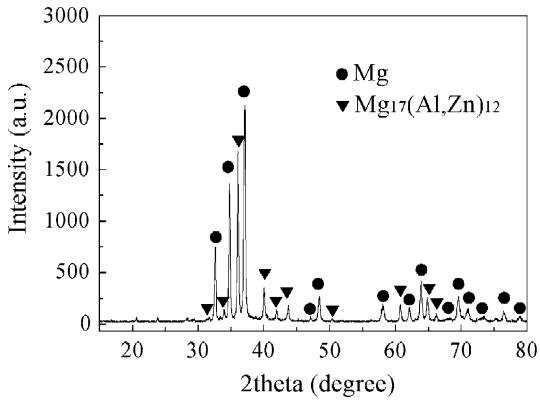

Fig. 6 XRD pattern of the brazing metal

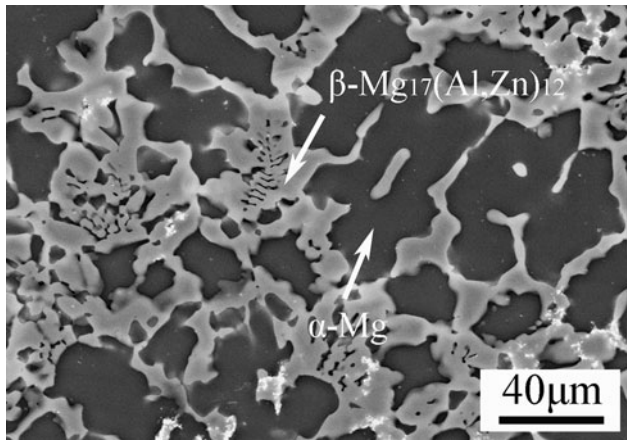

Fig. 7 SEM backscattered electron image of the brazing metal

showing the brazing metal consists of α-Mg and β-Mg_{17}(Al, $Zn)_{12}$ phases. The backscattered electron image of the brazing metal in the center of brazing region is shown in Fig. 7. The coarse β-Mg_{17}(Al, $Zn)_{12}$ phase is distributed at the boundary of the black α-Mg grains. The EDS analysis indicates that α-Mg solid solution contains Zn and Al elements. Compared with phase constitution in the original filler metal, it can be seen that the intensive alloying between the molten Al-Mg-Zn filler metal and the solid base metal AZ31B occurred in the brazing process and the homogeneous Mg_{32}(Al, $Zn)_{49}$ phase in the original filler metal is consumed after the brazing process.

3.4 Fracture Morphology of the Brazed Joint

The tensile test results indicate that the average of the shear strength is 35 MPa for the brazed joint. The microhardness value of the α-Mg and β-Mg_{17}(Al, $Zn)_{12}$ phases is 109 and 177 HV, respectively. The results indicate that the microhardness value of β-Mg_{17}(Al, $Zn)_{12}$ phase is much higher than that of α-Mg phase. Therefore, the microhardness between α-Mg and β-Mg_{17}(Al, $Zn)_{12}$ phases is discontinuous for the brazed joint. The fracture morphology of the brazed joint is shown in Fig. 8. The fracture surface of the brazed joint presents brittle fracture pattern. There is no evidence of ductile fracture such as dimples on the fracture surface of the brazed joint. The fracture morphology of the longitudinal cross section of the brazed joint

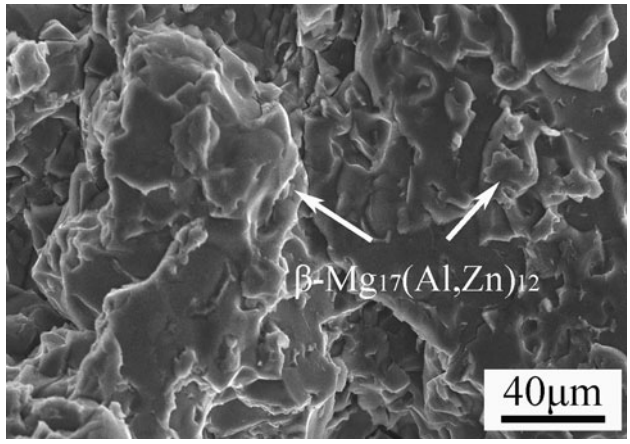

Fig. 8 SEM fracture morphology of the brazed joint

is shown in Fig. 9. From Fig. 9, it is indicated that fracture of the brazed joint exhibits intergranular fracture feature. The crack was originated from β-Mg_{17}(Al, $Zn)_{12}$ phase. Stress concentration is created easily from the hard β-Mg_{17}(Al, $Zn)_{12}$ phase when there is an external force acting on the brazed joint. With the effect of stress concentration, the hard β-Mg_{17}(Al, $Zn)_{12}$

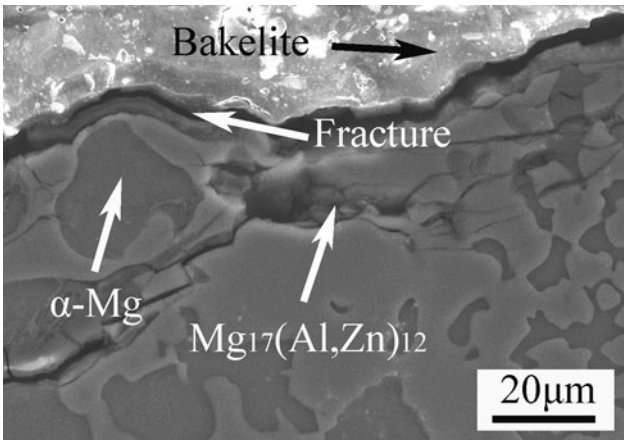

Fig. 9 SEM fracture morphology of the longitudinal cross section of the brazed joint

phase would be the weakest part in the brazed joint. Whereas, Zn and Al elements dissolved in α-Mg solid solution make an effect of solid-solution strengthening. As a result, the crack of the brazed joint would not originate from α-Mg solid solution.

4. Conclusions

Magnesium alloy AZ31B plates can be successfully brazed by means of high-frequency induction brazing with an Al-Mg-Zn filler metal. XRD test indicates that the brazing region consists of α-Mg and β-$Mg_{17}(Al, Zn)_{12}$ phases. It is found that the homogeneous $Mg_{32}(Al, Zn)_{49}$ phase in the original filler metal was consumed after the brazing process due to the intensive alloying between the molten filler metal and base metal in the process of brazing. The average of the shear strength is 35 MPa for the brazed joint. The fracture morphology of the brazed joint exhibits intergranular fracture mode and the crack originates from β-$Mg_{17}(Al, Zn)_{12}$ hard phase.

Acknowledgment

The authors acknowledge gratefully the financial support from the Beijing Municipal Education Commission, China (KM200710005005).

References

1. Y. Liu and X. Wu, A Microstructure Study on an AZ31 Magnesium Alloy Tube after Hot Metal Gas Forming Process, *J. Mater. Eng. Perform.*, 2007, **16**(3), p 354–359
2. J.W. Liu, D. Chen, Z.H. Chen, and H.G. Yan, Deformation Behavior of AZ31 Magnesium Alloy During Tension at Moderate Temperatures, *J. Mater. Eng. Perform.*, 2009, **18**(7), p 966–972
3. N. Afrin, D.L. Chen, X. Cao, and M. Jahazi, Strain Hardening Behavior of a Friction Stir Welded Magnesium Alloy, *Scripta Mater.*, 2007, **57**(11), p 1004–1007
4. S.H.C. Park, Y.S. Sato, and H. Kokawa, Effect of Micro-texture on Fracture Location in Friction Stir Weld of Mg Alloy AZ61 during Tensile Test, *Scripta Mater.*, 2003, **49**(2), p 161–166
5. L. Commin, M. Dumont, J.E. Masse, and L. Barrallier, Friction Stir Welding of AZ31 Magnesium Alloy Rolled Sheets: Influence of Processing Parameters, *Acta Mater.*, 2009, **57**(2), p 326–334
6. L.M. Liu, Z.D. Zhang, G. Song, and L. Wang, Mechanism and Microstructure of Oxide Fluxes for Gas Tungsten Arc Welding of Magnesium Alloy, *Metall. Mater. Trans. A*, 2007, **38A**(3), p 649–658
7. L.M. Liu and C.F. Dong, Gas Tungsten-arc Filler Welding of AZ31 Magnesium Alloy, *Mater. Lett.*, 2006, **60**(17–18), p 2194–2197
8. Z.D. Zhang, L.M. Liu, Y. Shen, and L. Wang, Mechanical Properties and Microstructures of a Magnesium Alloy Gas Tungsten Arc Welded with a Cadmium Chloride Flux, *Mater. Charact.*, 2008, **59**(1), p 40–46
9. P. Liu, Y.J. Li, H.R. Geng, and J. Wang, Microstructure Characteristics in TIG Welded Joint of Mg/Al Dissimilar Materials, *Mater. Lett.*, 2007, **61**(6), p 1288–1291
10. A. Munitz, C. Cotler, A. Stern, and G. Kohn, Mechanical Properties and Microstructure of Gas Tungsten Arc Welded Magnesium AZ91D Plates, *Mater. Sci. Eng. A*, 2001, **302**(1), p 68–73
11. T.P. Zhu, Z.W. Chen, and W. Gao, Microstructure Formation in Partially Melted Zone During Gas Tungsten Arc Welding of AZ91Mg Cast Alloy, *Mater. Charact.*, 2008, **59**(11), p 1550–1558
12. P. Liu, Y.J. Li, H.R. Geng, and J. Wang, A Study of Phase Constitution Near the Interface of Mg/Al Vacuum Diffusion Bonding, *Mater. Lett.*, 2005, **59**(16), p 2001–2005
13. L.M. Liu, J.H. Tan, and X.J. Liu, Reactive Brazing of Al Alloy to Mg Alloy Using Zinc-Based Brazing Alloy, *Mater. Lett.*, 2007, **61**(11-12), p 2373–2377
14. R.S. Coelho, A. Kostka, H. Pinto, S. Riekehr, M. Kocak, and A.R. Pyzalla, Microstructure and Mechanical Properties of Magnesium Alloy AZ31B Laser Beam Welds, *Mater. Sci. Eng. A*, 2008, **485**(1–2), p 20–30
15. Y.J. Quan, Z.H. Chen, X.S. Gong, and Z.H. Yu, CO_2 Laser Beam Welding of Dissimilar Magnesium-Based Alloys, *Mater. Sci. Eng. A*, 2008, **496**(1–2), p 45–51
16. Y.J. Quan, Z.H. Chen, Z.H. Yu, X.S. Gong, and M. Li, Characteristics of Laser Welded Wrought Mg-Al-Mn Alloy, *Mater. Charact.*, 2008, **59**(12), p 1799–1804
17. L.M. Liu, H.Y. Wang, and Z.D. Zhang, The Analysis of Laser Weld Bonding of Al Alloy to Mg Alloy, *Scripta Mater.*, 2007, **56**(6), p 473–476
18. C.T. Chi, C.G. Chao, T.F. Liu, and C.H. Lee, Aluminum Element Effect for Electron Beam Welding of Similar and Dissimilar Magnesium-Aluminum-Zinc Alloys, *Scripta Mater.*, 2007, **56**(9), p 733–736
19. C.T. Chi, C.G. Chao, T.F. Liu, and C.C. Wang, A Study of Weldability and Fracture Modes in Electron Beam Weldments of AZ Series Magnesium Alloys, *Mater. Sci. Eng. A*, 2006, **435–436**, p 672–680
20. T. Watanabe, S. Komatsu, and K. Oohara, Development of Flux and Filler Metal for Brazing Magnesium Alloy AZ31B, *Weld. J.*, 2005, **84**(3), p 37–40
21. B. Wielage and S. Mücklich, Improving the Soldering of Magnesium Alloys, *Weld. J.*, 2006, **85**(9), p 48–51
22. S. Muecklich, G. Fritsche, and B. Wielage, Amorphous Filler Metals Offer Great Potential for Joining Magnesium Alloys, *Weld. J.*, 2008, **87**(3), p 31–33
23. T. Watanabe, S. Komatsu, and K. Oohara, Development of Flux and Filler Metal for Brazing Magnesium Alloy AZ31B, *Weld. J.*, 2005, **84**(3), p 37–40